Improved Impacts in Observing System Simulation Experiments of Radio Occultation Observations as a Result of Model and Data Assimilation Changes

L. CUCURULL[a] AND S. P. F. CASEY[b,a]

[a] *NOAA/Atlantic Oceanographic and Meteorological Laboratory, Miami, Florida*
[b] *Cooperative Institute for Marine and Atmospheric Studies, University of Miami, Miami, Florida*

(Manuscript received 28 May 2020, in final form 5 November 2020)

ABSTRACT: As global data assimilation systems continue to evolve, observing system simulation experiments (OSSEs) need to be updated to accurately quantify the impact of proposed observing technologies in weather forecasting. Earlier OSSEs with radio occultation (RO) observations have been updated, and the impact of the originally proposed Constellation Observing System for Meteorology, Ionosphere and Climate-2 (COSMIC-2) mission, with high-inclination and low-inclination components, has been investigated by using the operational data assimilation system at NOAA and a one-dimensional bending-angle RO forward operator. It is found that the impact of the low-inclination component of the originally planned COSMIC-2 mission (now officially named COSMIC-2) has significantly increased as compared with earlier studies, and significant positive impact is now found globally in terms of mass and wind fields. These are encouraging results as COSMIC-2 was successfully launched in June 2019 and data have been recently released to operational weather centers. Earlier findings remain valid indicating that globally distributed RO observations are more important to improve weather prediction globally than a denser sampling of the tropical latitudes. Overall, the benefits reported here from assimilating RO soundings are much more significant than the impacts found in previous OSSEs. This is largely attributed to changes in the data assimilation and forecast system and less to the more advanced one-dimensional forward operator chosen for the assimilation of RO observations.

KEYWORDS: Numerical weather prediction/forecasting; Data assimilation; Remote sensing

1. Introduction

After the success of the Constellation Observing System for Meteorology, Ionosphere and Climate (COSMIC) mission (Anthes et al. 2008) in improving global numerical weather prediction (NWP) forecasts at NOAA (Cucurull 2010; Cucurull et al. 2013; Cucurull and Anthes 2014), the United States, in partnership with Taiwan, developed a follow-on COSMIC-2 mission. Although originally planned to include six satellites in low-inclination orbits (equatorial component) and six satellites in high-inclination orbits (polar component) to be launched within 18 months of the first (equatorial) launch, the United States and Taiwan decided to move forward with the equatorial component only. The six satellites in equatorial orbit included instruments for space-weather applications and were planned to provide a significant number of radio-occultation (RO) soundings for tropical cyclone applications. The six COSMIC-2 satellites were successfully launched from Kennedy Space Center in Cape Canaveral, Florida, on 24 June 2019. The final orbit configuration is expected to be achieved around May of 2021. COSMIC-2 should provide ~6000 profiles per day with better instrument performance than COSMIC, particularly in the lower moist tropical troposphere, due to a higher antenna gain.

In preparation for the launch of COSMIC-2, NOAA conducted a series of observing system simulation experiment (OSSE) studies to quantify the impact of RO observations in NWP from the two components of the originally planned COSMIC-2 mission. OSSEs are numerical weather experiments that allow one to cost-effectively quantify the impact of satellite observing systems before they are deployed in space. We refer to Hoffman and Atlas (2016) for a detailed description of the OSSE method. Very briefly, an OSSE consists of a free-running NWP model that provides an accurate representation of the climatology of the atmosphere, typically called the *nature run* (NR). Current and proposed observations, with their associated error characteristics, are then simulated from the NR. Rigorous validation and calibration of the OSSE system are necessary to ensure realistic results, and any limitations of the system need to be determined and documented. For example, is the NR and the differences between the NR and the forecast model used in the experiments realistic? Are the coverage and error characteristics of simulated observations appropriate? Are the forecast accuracy and impacts of existing observing systems in the OSSE comparable to real world? Ultimately, conclusions of an OSSE should not be drawn beyond the limitations of the study.

All of the global OSSEs with COSMIC-2 conducted at NOAA over the past several years assumed final orbit satellite configuration for both the low- and high-inclination orbits, with total counts of ~12 000 profiles per day (Cucurull et al. 2017, 2018). The most recent study was conducted by Cucurull and Mueller (2020), who investigated the impact of the two components of the originally planned COSMIC-2 mission, both independent and combined. In addition, that study investigated trade-offs in the design of the high-inclination component. In particular, the number of RO soundings,

Corresponding author: L. Cucurull, lidia.cucurull@noaa.gov

DOI: 10.1175/MWR-D-20-0174.1

© 2021 American Meteorological Society. For information regarding reuse of this content and general copyright information, consult the AMS Copyright Policy (www.ametsoc.org/PUBSReuseLicenses).

Brought to you by NOAA Central Library | Unauthenticated | Downloaded 01/25/21 09:15 PM UTC

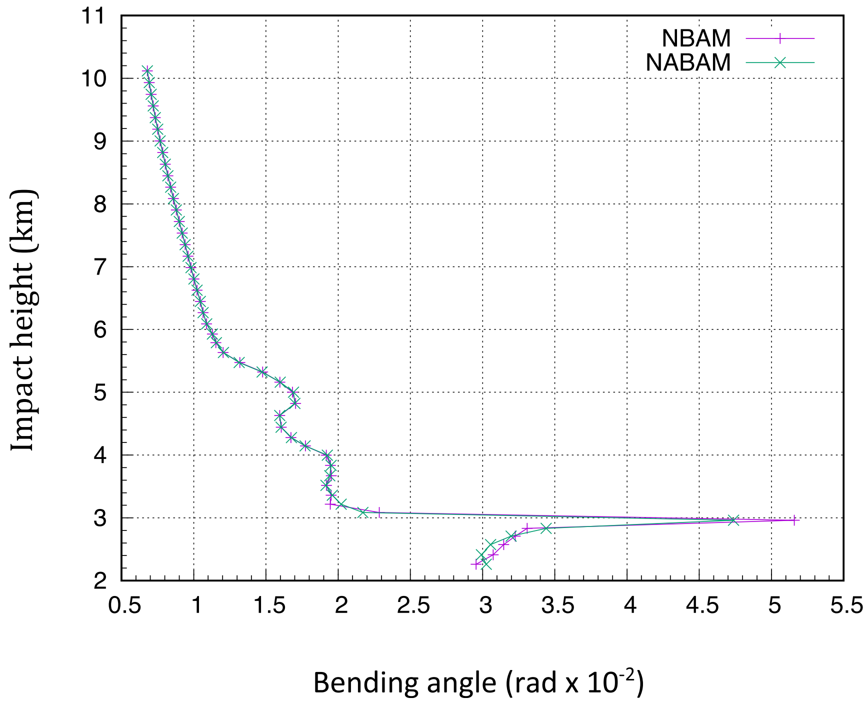

FIG. 1. Simulated bending-angle profile (radians $\times 10^{-2}$) as a function of the impact height (km) with current (NBAM) and enhanced (NABAM) methods.

their accuracy, and spatial coverage were analyzed. The potential benefits from COSMIC-2 were investigated by using profiles of refractivity as the RO observation type. However, the operational global data assimilation system at NOAA uses bending-angle observations, a less derived quantity than refractivity. The reader is referred to Melbourne et al. (1994), Kursinski et al. (1997), and Rocken et al. (1997) for a detailed description of the RO technology and retrieval algorithms.

To confirm some of the earlier results obtained with the assimilation of refractivity and ensure robustness of the findings, we repeated some of the COSMIC-2 experiments but assimilated soundings of bending angle rather than refractivity, as well as used the current research version of the global data assimilation and forecast system at NOAA. This work focuses on quantifying impacts from the originally planned COSMIC-2 mission using the most recent NWP configuration and RO observation type used at NOAA and compares those results with earlier studies. Although RO plays an important role in bias-correction of satellite radiances by preventing model drifting toward its own biased climate (Dee 2005; Cucurull et al. 2014; Bonavita 2014), this is not investigated here.

The paper is structured as follows: section 2 describes the experiment setup, including the OSSE system configuration and the experiments conducted in this study. Section 3 presents the impact of the low- and high-inclination orbit components, independently and combined. Section 4 discusses how these results compare with earlier OSSEs with refractivity and an earlier version of the NOAA's operational global data assimilation and forecast system. Section 5 summarizes the main conclusions.

2. Experiment setup

The OSSE system used to conduct the experiments includes a 2-yr nature run based on the 7-km-resolution, nonhydrostatic NASA Global Modeling and Assimilation Office (GMAO) Goddard Earth Observing System Model, version 5 (GEOS-5; Putman et al. 2014, 2015). Calibration of this OSSE system was conducted in 2015 based on the August–September 2014 operational observing system architecture. Conventional and clear-sky satellite radiance observations were simulated from the nature run for the August–September time period (Boukabara et al. 2018).

The OSSE system used in this study differs from earlier investigations in two ways. First, RO observations were simulated using a bending-angle forward operator rather than a refractivity forward operator. For this purpose, profiles of bending angle were simulated using a slightly modified version of the operational RO forward operator, the National Centers for Environmental Prediction (NCEP) bending-angle method (NBAM; Cucurull et al. 2013). The enhanced method, the NCEP advanced bending-angle model (NABAM), simulates observations in the lower moist troposphere more accurately than with the operational NBAM, in particular in cases of large vertical gradients of atmospheric refractivity (Cucurull et al. 2020). Limitations associated with the simulation of bending-angle observations in the lower troposphere under super-refraction or ducting conditions are partially eliminated in

Brought to you by NOAA Central Library | Unauthenticated | Downloaded 01/25/21 09:15 PM UTC

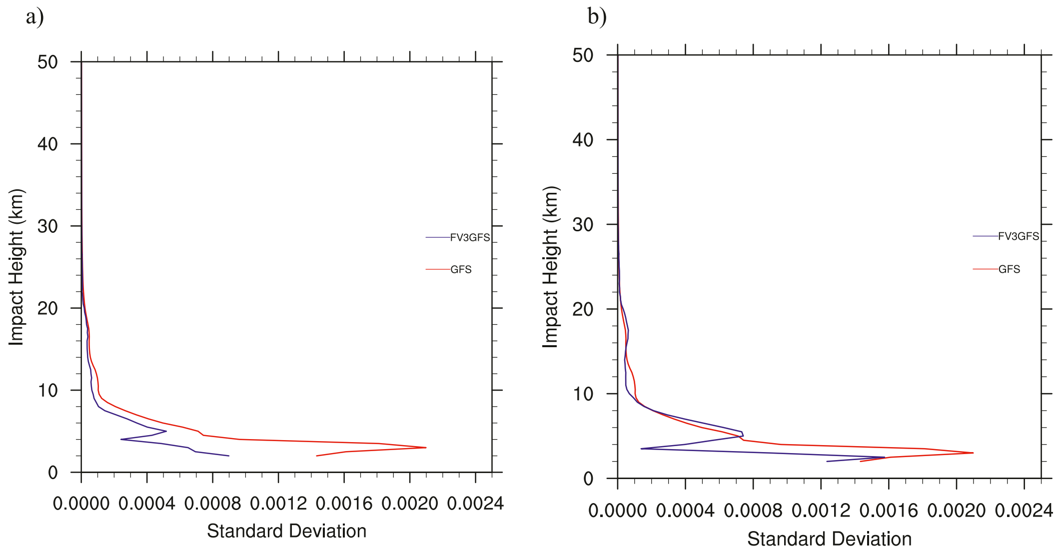

FIG. 2. Bending-angle standard deviations (radians) as a function of the impact height (km) used in the GFS (red) and FV3GFS (blue) OSSE systems for (a) polar and (b) equatorial COSMIC-2 satellites. Standard deviations were calculated from the observation increments (observation − background) from the real and OSSE experiments for a 2-week period on the basis of the 2019 RO satellite configuration in the FV3GFS system and the 2014 RO satellite configuration in the GFS system, and the specific explicit error was added to the simulated observations. This error includes measurement, representativeness, and forward-model errors.

NABAM by a reformulation of the forward operator that has no adverse effects at higher altitudes. As an example, Fig. 1 shows the simulation of a single bending-angle profile with NBAM and NABAM methods for the lowest 10 km of the atmosphere in a case where large vertical gradients of refractivity existed. Simulations with NABAM and NBAM differ slightly below ~4 km.

The second main difference with earlier COSMIC-2 impact studies is that we adopted NCEP's current operational data assimilation and forecast system, with a finite-volume cubed-sphere dynamical core (FV3) and the four-dimensional ensemble variational (4DEnVar) version of the NCEP's grid-point statistical interpolation analysis. Following guidelines to conduct research at NCEP, the experiments used a lower horizontal resolution system that aims to mimic the operational data assimilation and forecast system as closely as possible. The forecast model was run at a resolution of C384 (~25 km), and the analysis is at a resolution of T254 (~50 km). Twenty (80 in the operational configuration) reduced-resolution T254L64 ensemble members were generated for use in estimating the hybrid background error covariance via the ensemble Kalman filter. The 64 vertical levels are the same as in the operational configuration for all components of the data assimilation system. In contrast to earlier studies, the operational RO assimilation algorithms and existing quality control procedures were used to assimilate COSMIC-2 observations. As in the operational configuration, RO observations above 50 km were not used.

Earlier experiments used the Global Forecast System (GFS) dynamical core and were run with the 2015 operational configuration at the research resolution of ~27 km for the model forecasts and used a hybrid three-dimensional (3D) ensemble variational (EnVar) analysis at a resolution of T254 (~50 km). Eighty reduced-resolution T254L64 ensemble members were generated to estimate background error covariance via the ensemble Kalman filter. As with the FV3 system, the number of vertical layers was kept the same as in the operational configuration (64). The FV3 dynamical core replaced NOAA's legacy GFS dynamical core in early 2019, and the new system is typically referred to as FV3GFS or FV3.

Errors were added to all the simulated observations following the method described in Errico et al. (2013), in which observation errors are tuned in the OSSE system to match the corresponding statistics with real observations. Figure 2 shows the final tuned errors in the FV3GFS system for the simulated RO observations from the polar and equatorial COSMIC-2 orbit configurations. Errors were estimated from the observation increments for a two-week period and the specific explicit error was added to the simulated perfect observations. This error includes measurement, representativeness, and forward-model errors. Horizontal correlated observation errors were not included in either the simulation or assimilation processes for any of the observations, including RO. A correlation scale of 0.5 km was used to generate vertical correlated errors for RO observations.

To compare results between the FV3GFS and GFS OSSE systems, calibration of the FV3GFS/G5NR OSSE system was conducted with the observing system of 2014, so the same observations were used. Experiments with real (FV3GFS) and simulated (FV3GFS OSSE) observations ran from 1 August to 30 September 2014, and the first two weeks were used for model spinup. Both experiments assimilated RO observations. As an example, results for the anomaly correlation score for the 500-hPa geopotential heights and for the 200-hPa root-mean-square

Brought to you by NOAA Central Library | Unauthenticated | Downloaded 01/25/21 09:15 PM UTC

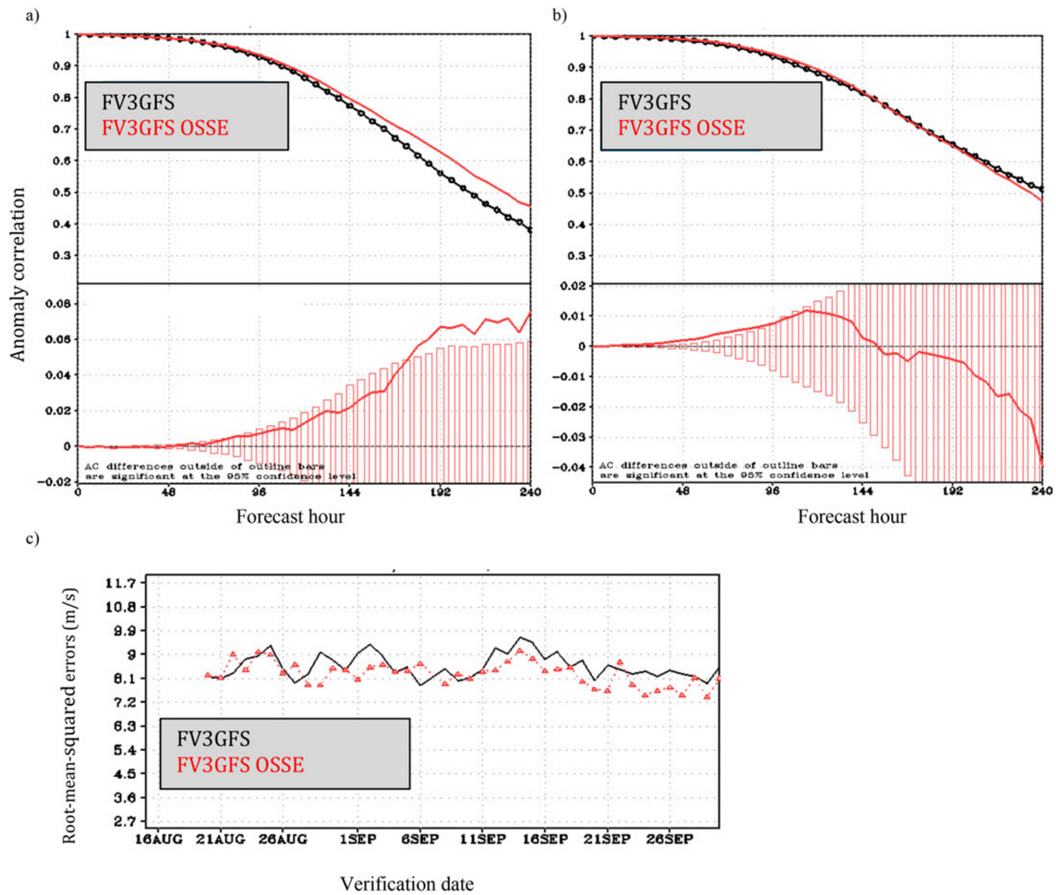

FIG. 3. Predictability of the FV3GFS OSSE and operational FV3GFS systems for the 2014 observing system. Anomaly correlation scores for the 500-hPa geopotential heights as a function of the forecast lead time are shown for the (a) Northern Hemisphere and (b) Southern Hemisphere. The lower parts of each panel show differences between FV3GFS OSSE and FV3GFS, with positive being an improvement. Bars show limits of statistical significance at the 95% confidence level; values outside the bars are statistically significant. Also shown are (c) root-mean-square errors for the 200-hPa tropical winds (m s^{-1}) at day 5. Experiments are run from 1 Aug to 30 Sep 2014, and the verification was conducted for 15 Aug–30 Sep; RO observations were included in the experiments.

(RMS) wind error are shown in Figs. 3a–c. Although the OSSE system shows higher predictability than the real world for the 500-mb geopotential heights anomaly correlation score in the extratropics (Figs. 3a,b) and for the upper level winds in the tropical latitudes (Fig. 3c), overall it produces slightly more comparable results than the earlier GFS/G5NR global OSSE system (Casey et al. 2019). Specific calibration of the RO component of the OSSE system is provided in Fig. 4, showing that the accuracy and impact of simulated RO observations in the OSSE system are comparable to their values in the real world (FV3GFS). Individual calibration of each component of the global observing system was not performed.

Low-inclination (equatorial) and high-inclination (polar) COSMIC-2 bending-angle profiles were simulated using the enhanced NABAM RO forward operator. A total of ~12 000 profiles (6000 equatorial and 6000 polar) were simulated daily. Spatial coverage of equatorial and polar bending-angle observations assimilated in a 6-h time window is shown in Fig. 5. As in earlier OSSE studies with COSMIC-2 observations, transmitting satellites from both the U.S. Global Positioning System (GPS) and the Russian Global Navigation Satellite System (GLONASS) constellations were included in the simulation of RO profiles.

A NOROCONTROL simulation experiment assimilated all of the conventional and satellite radiance observations operationally that were assimilated in 2014, except for RO observations (Table 1). Simulated low-inclination (equatorial) RO bending angles were added to the NOROCONTROL in the COSMIC-2 Equatorial Experiment (C2EQE), and high-inclination (polar) bending angles were added in the COSMIC-2 Polar Experiment (C2POE). Finally, both equatorial and polar RO observations were assimilated in the COSMIC-2 Equatorial and Polar Experiment (C2EQPOE). A list of the experiments conducted in this study is summarized in Table 2. All of the experiments ran from 1 August to 30 September 2006, and, as in the operational configuration, we used a 6-h data assimilation time window as the cycling interval. However, because of limited computing resources, we only

Brought to you by NOAA Central Library | Unauthenticated | Downloaded 01/25/21 09:15 PM UTC

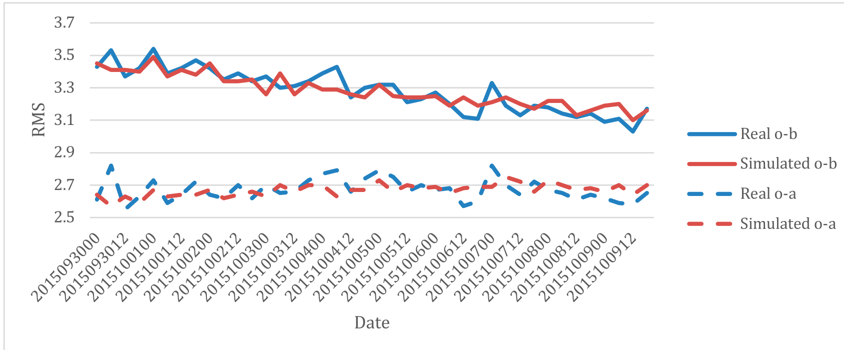

FIG. 4. Time series of the root-mean-square normalized innovation (percentage) of the bending angle. Solid lines show observation minus background (aka innovations), and dashed lines show observations minus analysis in the operational FV3GFS (blue) and FV3GFS OSSE (red) systems. Statistics are shown for the 2015 RO data.

produced once-daily extended 240-h global forecasts initialized at 0000 UTC, in contrast to the four daily extended forecasts produced in the operational configuration. The first month was used for model spinup and verification against the NR was done for 1–30 September 2006. All forecast skill metrics are calculated with respect to the nature run. Statistical significance of the differences between experiments is calculated with the Student's t test. The NCEP's statistical verification package, which is used in our experiments, doesn't account for serial correlation among the forecasts, so actual confidence levels are expected to be slightly lower than the 95% reported in the figures.

3. Radio occultation impact sensitivity to geographical data distribution

The anomaly correlation skill in the Northern Hemisphere extratropics (NH; 20°–80°N) for the 250-, 500-, and 700-hPa geopotential heights as a function of the forecast length are shown in Figs. 6a, 6c, and 6e, respectively. The denser equatorial coverage in C2EQE results in an overall slightly positive impact as compared to the control experiment (NOROCONTROL). Differences with respect to the control experiment are positive and, in general, statistically significant during the first 5 days. A slightly positive impact of C2POE over C2EQE is found during the first 5 days. Differences between C2POE and NOROCONTROL are statistically significant up to around day 5. The largest benefits in the NH from assimilating RO are found when the number of observations is the highest, and soundings are globally distributed in experiment C2EQPOE. Differences between C2EQPOE and NOROCONTROL are statistically significant until around day 7.

Corresponding plots for the Southern Hemisphere extratropics (SH; 20°–80°S) are shown in Figs. 6b, 6d, and 6f. The impact of assimilating observations with denser equatorial coverage (C2EQE) is slightly larger in the SH than in the NH, and differences with respect to the NOROCONTROL are now statistically significant until a larger forecast lead time (day 6). Experiments C2EQPOE and C2POE have similar and larger skill than C2EQE, and differences between C2EQPOE and NOROCONTROL extend to longer lead times. The result that both C2EQPOE and C2POE tend to show similar skill at

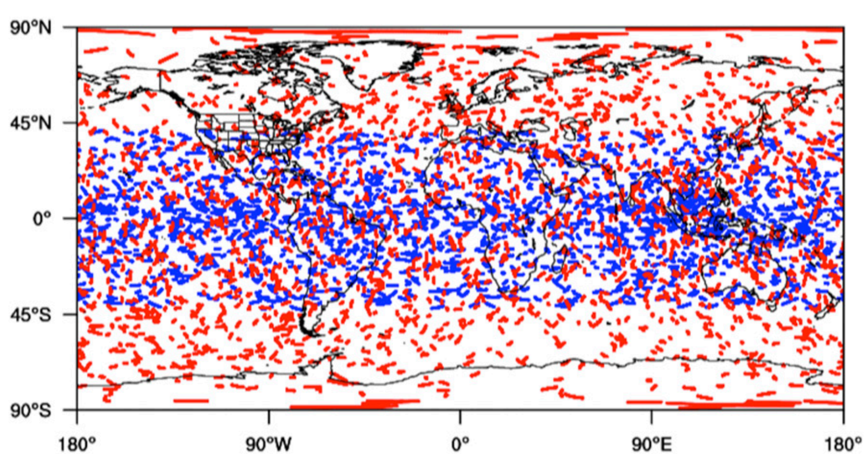

FIG. 5. Spatial distribution of the COSMIC-2 observations from the equatorial (blue) and the polar (red) configurations for a 6-h assimilation time window.

Brought to you by NOAA Central Library | Unauthenticated | Downloaded 01/25/21 09:15 PM UTC

TABLE 1. Observations used operationally at NCEP as of 2014 and assimilated in the NOROCONTROL experiment [after Table 1 of Cucurull and Mueller (2020)].

Observation type	Observations
Surface pressure	Rawinsonde, surface marine, surface land, dropsonde, and surface METAR
Wind	Rawinsonde, pilot balloon (PIBAL), NOAA Profiler Network (NPN) wind profiler, VAD profiles, wind profiler-PIBAL decoded, aircraft, dropsonde, aircraft, JMA/Himawari, EUMETSAT/Meteosat, NOAA/GOES, MODIS (*Aqua*), surface marine, and ASCAT
Temperature	Rawinsonde, aircraft, aircraft, surface marine, and dropsonde
Moisture	Rawinsonde, dropsonde, and surface marine
Radiance	*Metop-A* (HIRS4, AMSU-A, MHS, IASI), *Metop-B* (AMSU-A,MHS, IASI), *GEOS-15* (Sounders 1–4), *Suomi -NPP* (ATMS, CriS), *Aqua* (AIRS, AMSU-A), *N15* (AMSU-A), *N18* (AMSU-A, MHS), *N19* (AMSU-A, MHS), *F17* (SSMIS), *F18* (SSM/IS), and *M10* (SEVIRI)

the different vertical ranges of the atmosphere suggests that adding more RO data in the tropical regions than already available in C2POE does not result in significant additional benefits in terms of this metric. Overall, the benefits from the assimilation of RO observations in C2POE are slightly larger in the SH than in the NH, while these benefits are comparable for experiment C2EQPOE.

From these results, the impact of RO in the NH for the midterm forecasts (days 3–6) is more beneficial when soundings are globally uniformly distributed, and when the number of RO observations is larger. As in previous studies, results suggest that uniform geographical data coverage is more beneficial in the extratropics than having high density data coverage over tropical latitudes. In the SH, denser data coverage in the 40°S–40°N latitudinal band is more beneficial than in the NH, and benefits further increase, and remain higher than in the NH, when the data are globally uniformly distributed. Unlike what is observed in the NH, there is no additional benefit gained when sampling is increased over the tropical latitudes beyond what is already sampled in C2POE.

When compared with the findings from Cucurull and Mueller (2020), which used the 2015 version of the NCEP's operational data assimilation and forecast system and a different RO forward operator, the impact of the equatorial segment (C2EQE) is significantly larger in both the NH and SH. Earlier OSSEs showed neutral impact in the NH and neutral to slightly negative impact in the SH. The largest benefits found in Cucurull and Mueller (2020) with the assimilation of both equatorial and polar COSMIC-2 segments combined remain valid, but the benefits over a control experiment without RO observations are larger with the new FV3GFS data assimilation and forecast system and a more advanced bending-angle forward operator, especially in the NH.

Global upper level RMS wind errors are shown in Figs. 7a, 7c, and 7e. In the NH (Fig. 7a), a reduction in 200-hPa RMS wind errors is found with the assimilation of RO observations in all three experiments. As for the mass field, benefits increase from C2EQE to C2POE during the first 6 days, and these benefits are largest when a higher number of RO observations are assimilated in C2EQPOE (reduction of 1.2 m s^{-1} relative to NOROCONTROL at day 4). Overall, differences between the RO experiments and NOROCONTROL are statistically significant up to day 6 for C2EQE and C2POE and up to day 9 for C2EQPOE. Similarly, all three RO experiments reduce wind errors in the tropical latitudes (Fig. 7c), although there is more variability to which experiment produces the largest benefits. During the first 48 h of the forecast, C2EQPOE gives the largest wind error reduction (0.85 m s^{-1} at the analysis time) but results are more mixed afterward. Overall, differences between the RO experiments and the control are statistically significant until day 6 and, except for the first 48 h, error reduction is typically larger in the NH than in the tropics. All experiments with RO decrease upper-level RMS wind errors in the SH as well, with C2POE and C2EQPOE resulting in the largest error reduction for the entire forecast range. Differences with NOROCONTROL are statistically significant until day 6 in C2EQE and through the extended forecast range in C2POE and C2EQPOE. In general, the reduction of RMS error in all three RO experiments is more significant in the SH than in any other latitudinal range.

Although smaller in magnitude, RMS lower-level wind errors are also similarly improved with the assimilation of RO observations (Figs. 7b,d,f). As for the mass field, the benefits resulting from the assimilation of RO observations in reducing upper and lower-level RMS wind error is larger than the findings in Cucurull and Mueller (2020). The positive impact is now much larger and differences between the equatorial component and the control are statistically significant in the extratropics. Cucurull and Mueller (2020) had found neutral impact in wind error reduction in the extratropics with the

TABLE 2. Summary of the different experiments conducted in this study.

Expt name	C2 observations	Model	Observation type
NOROCONTROL	—	FV3GFS	—
C2EQE	Equatorial	FV3GFS	Bending angle
C2POE	Polar	FV3GFS	Bending angle
C2EQPOE	Equatorial + polar	FV3GFS	Bending angle
CTL_NORO	—	GFS	—
C2EQE_GFS	Equatorial	GFS	Bending angle
C2EQPOE_GFS	Equatorial + polar	GFS	Bending angle
C2EQE_NGFS	Equatorial	GFS	Refractivity
C2EQPOE_NGFS	Equatorial + Polar	GFS	Refractivity

Brought to you by NOAA Central Library | Unauthenticated | Downloaded 01/25/21 09:15 PM UTC

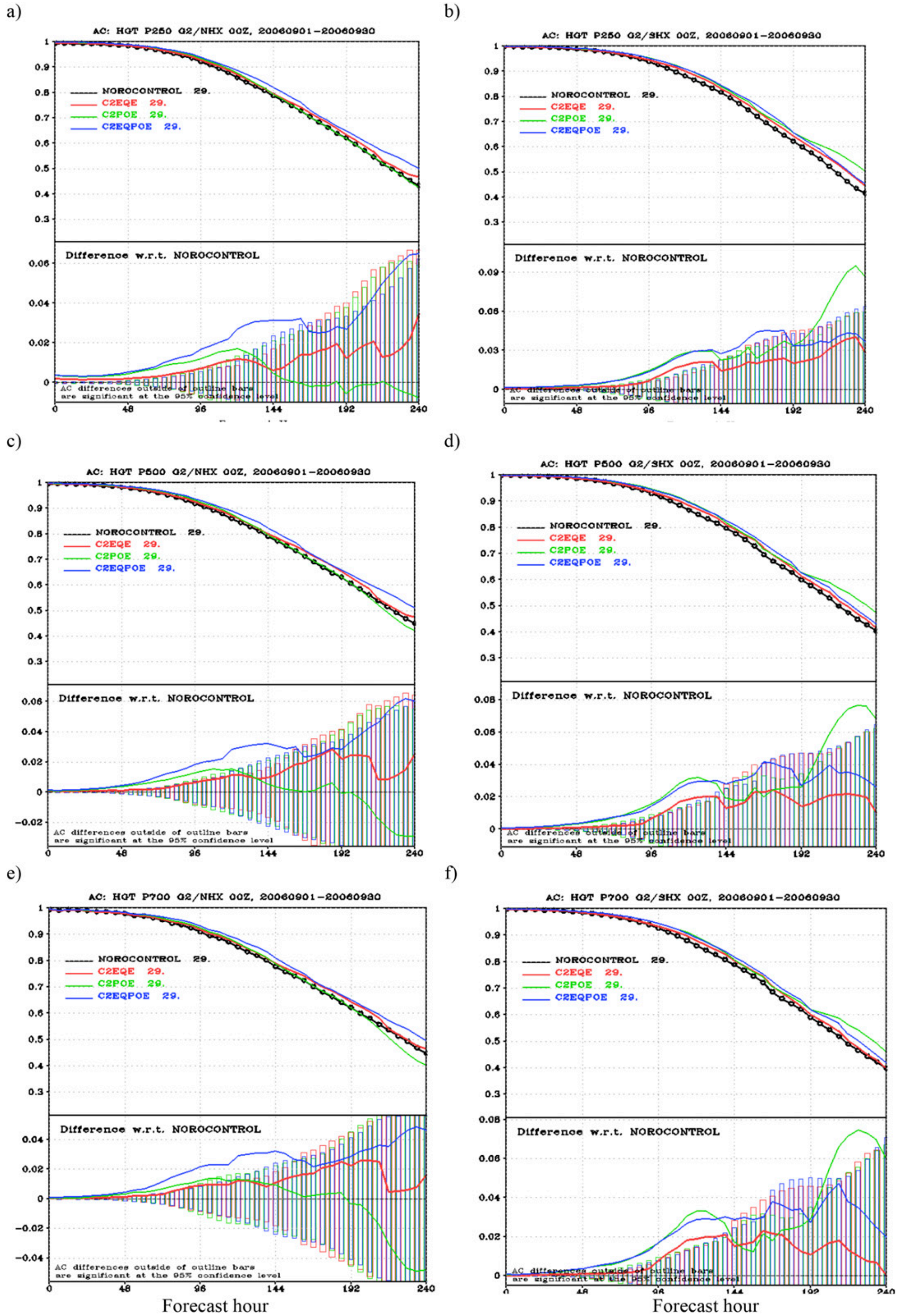

FIG. 6. Anomaly correlation score for the 250-, 500-, and 700-hPa geopotential heights for NOROCONTROL (black), C2EQE (red), C2POE (green), and C2EQPOE (blue) for (a),(c),(e) Northern Hemisphere and (b),(d),(f) Southern Hemisphere. The lower parts of each panel show differences with respect to NOROCONTROL, with positive being an improvement. Bars show limits of statistical significance at the 95% confidence level; values outside the bars are statistically significant.

Brought to you by NOAA Central Library | Unauthenticated | Downloaded 01/25/21 09:15 PM UTC

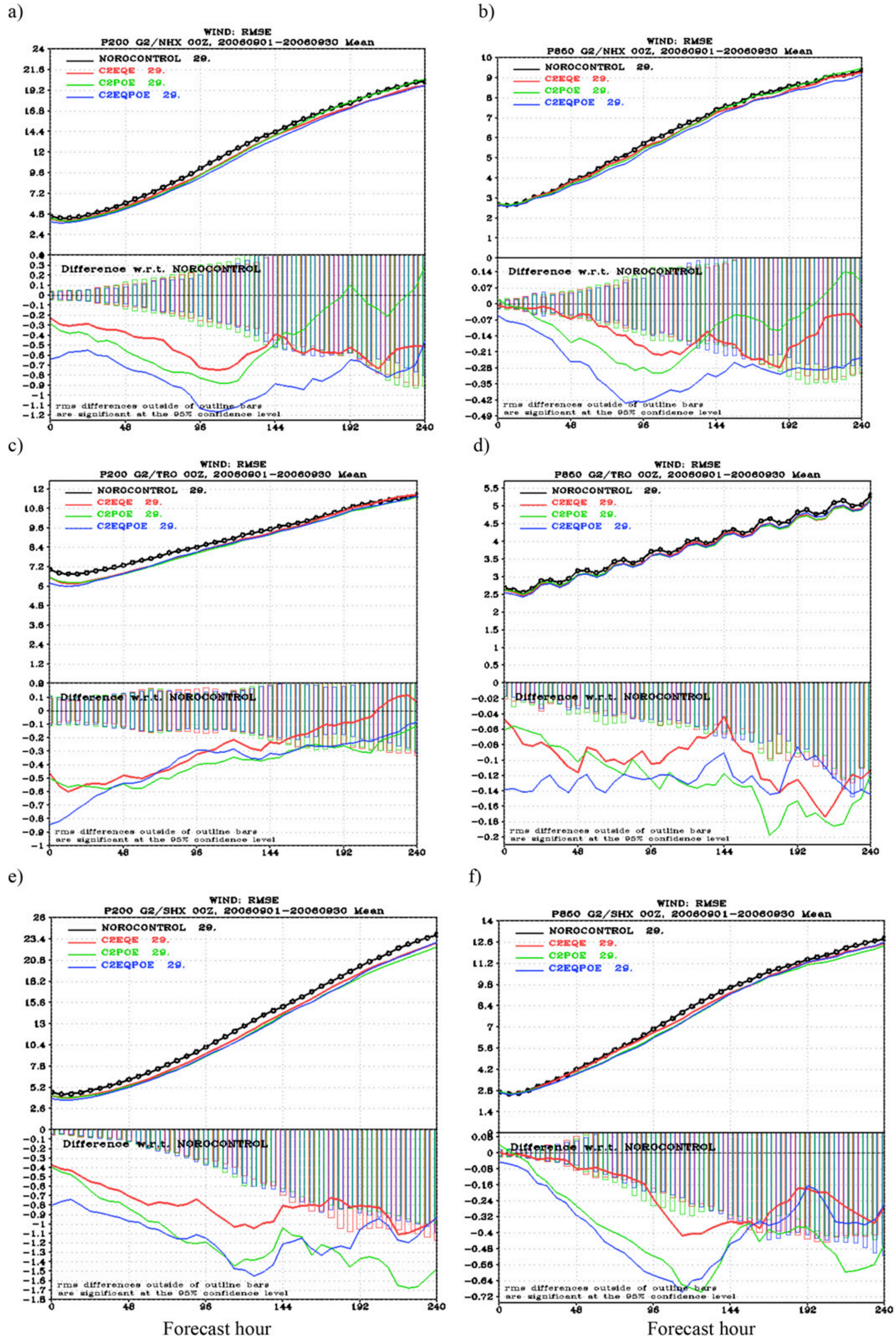

FIG. 7. (left) Upper (200 hPa) and (right) lower (850 hPa) root-mean-square wind errors (m s^{-1}) for the (a),(b) Northern Hemisphere; (c),(d) tropics; and (e),(f) Southern Hemisphere as a function of the forecast hour for NOROCONTROL (black), C2EQE (red), C2POE (green), and C2EQPOE (blue). The lower parts of each panel show differences with respect to NOROCONTROL, with negative being an improvement. Bars show limits of statistical significance at the 95% confidence level; values outside the bars are statistically significant.

Brought to you by NOAA Central Library | Unauthenticated | Downloaded 01/25/21 09:15 PM UTC

assimilation of COSMIC-2 equatorial observations. RMS wind error reduction values for the two OSSEs give similar in the tropics (20°S–20°N).

4. Sensitivity of OSSE results to changes in the data assimilation and forecast system

Results from the previous section confirm that the impact of RO has slightly changed from earlier studies. In this section, we quantify how changes in the NWP system and the type of RO observation, and associated forward operator, might have altered the results.

a. *Changes in the analysis and forecast model*

In section 3, we presented impact results for three RO satellite orbit configurations based on the original design of COSMIC-2. All experiments used a current version of the operational FV3GFS data assimilation and forecast system and a bending-angle forward operator. These results can be compared with earlier OSSEs conducted with an older version of NCEP's NWP system that was operational in 2015 (Q1FY15 version), while retaining a bending-angle forward operator for the simulation and assimilation of RO observations.

The NABAM simulator used to simulate bending angles in the FV3GFS OSSE system described in section 2 was used to generate synthetic bending-angle observations. Random errors were added to perfect bending angles and other observations following the same procedure described in Cucurull and Mueller (2020). As can be seen in Fig. 2, this iterative error estimation resulted in smaller RO errors for the FV3GFS OSSE configuration than when the GFS OSSE system was used. This is true for both the equatorial and polar RO observations and it seems to indicate that the FV3GFS system might have smaller representativeness errors than the older GFS configuration, potentially contributing to a larger impact from the assimilation of these observations.

We ran three additional OSSEs to test the sensitivity of the results to alterations of the data assimilation and forecast system (see Table 2). As with the FV3GFS experiments analyzed in section 3, all of the observations that were operationally assimilated in 2014, except for RO observations, were assimilated in a CTL_NORO experiment. Simulated equatorial COSMIC-2 RO bending-angle soundings were added to the CTL_NORO in C2EQE_GFS, and the polar observations were added to C2EQE_GFS in the C2EQPOE_GFS experiments. The impact of RO observations in C2EQE_GFS and C2EQPOE_GFS relative to a control run without RO observations should be compared with the impact results from C2EQE and C2EQPOE in section 3, respectively (There is no counterpart for the C2POE experiment.) The only difference between these experiments and those of section 3 is the data assimilation and forecast system, since RO observations were simulated with the same forward operator and errors were added to the perfect observations according to the values estimated for each OSSE configuration (Fig. 2).

Similar to the FV3GFS OSSE configuration, all of the experiments ran from 1 August to 30 September 2006, and verification against the G5NR was done for 1–30 September 2006. For this second set of experiments, once-daily extended 168-h global forecasts were initialized at 0000 UTC. (The research version of the 2015 NCEP's data assimilation and forecast system only extended to 168-h forecasts).

Figures 8a and 8b show the 500-hPa geopotential heights anomaly correlation score for the NH and SH, respectively. As in Figs. 6c and 6d, where the FV3GFS configuration was used, the impact of the equatorial and polar components combined is larger than the impact of the equatorial component alone. In the NH (Fig. 8a), the impact of the equatorial RO observations is overall neutral to slightly negative, while the impact is mostly neutral in the SH (Fig. 8b). Benefits from the full originally planned COSMIC-2 constellation remains marginal in the NH while a small benefit is found in the SH. Results presented in section 3 (Figs. 6c,d), where a more advanced data assimilation and forecast system was used, showed a much larger impact from the assimilation of RO observations. This is true for both the equatorial (C2EQE_GFS vs C2EQE) and both equatorial and polar observations combined (C2EQPOE_GFS vs C2EQPOE), and it is valid for both extratropical latitudinal bands. The impact of RO observations is not just higher in magnitude with the more advanced FV3GFS system, but also differences with the corresponding control experiment are also statistically significant. This result seems to suggest that the advanced FV3GFS data assimilation and forecast configuration, with improved assimilation algorithms and a new dynamical core, is capable of extracting more information from the bending-angle observations.

Overall reduced impact in the extratropics with an older version of the data assimilation and forecast system is found for the RMS wind errors as well. The use of the older data assimilation and forecast system shows overall neutral impact for the upper (Fig. 9a) and lower-level (Fig. 9b) RMS wind errors in the NH, while positive and statistically significant impact was found for both orbit configurations with the use of FV3GFS (Figs. 7a,b). Although a reduction in upper-level wind error is obtained in C2EQE_GFS and C2EQPOE_GFS in the SH (Fig. 9e), the impact is less significant than in C2EQE and C2EQPOE (Fig. 7e). The impact is also lower in magnitude for the lower-level winds in the SH, with neutral impact from the equatorial RO configuration in C2EQE_GFS and slightly positive impact in C2EQPOE_GFS (Fig. 9f). Larger benefits were found with the FV3GFS system for both RO satellite orbit configurations. Smaller differences between both data assimilation and forecast systems are observed in the tropical latitudes, although adding polar RO observations to the C2EQE_GFS equatorial component in C2EQPOE_GFS produces no further reduction in error for the lower-level winds (Fig. 9d). Positive impact was found when adding RO polar observations in the FV3GFS system (Fig. 7d).

b. *Changes in the radio occultation observation type*

COSMIC data became operationally assimilated at NCEP in 2007. A refractivity forward operator was initially used (Cucurull 2010), which was later replaced with a one-dimensional bending-angle forward operator in 2012 (Cucurull et al. 2013). Profiles of

Brought to you by NOAA Central Library | Unauthenticated | Downloaded 01/25/21 09:15 PM UTC

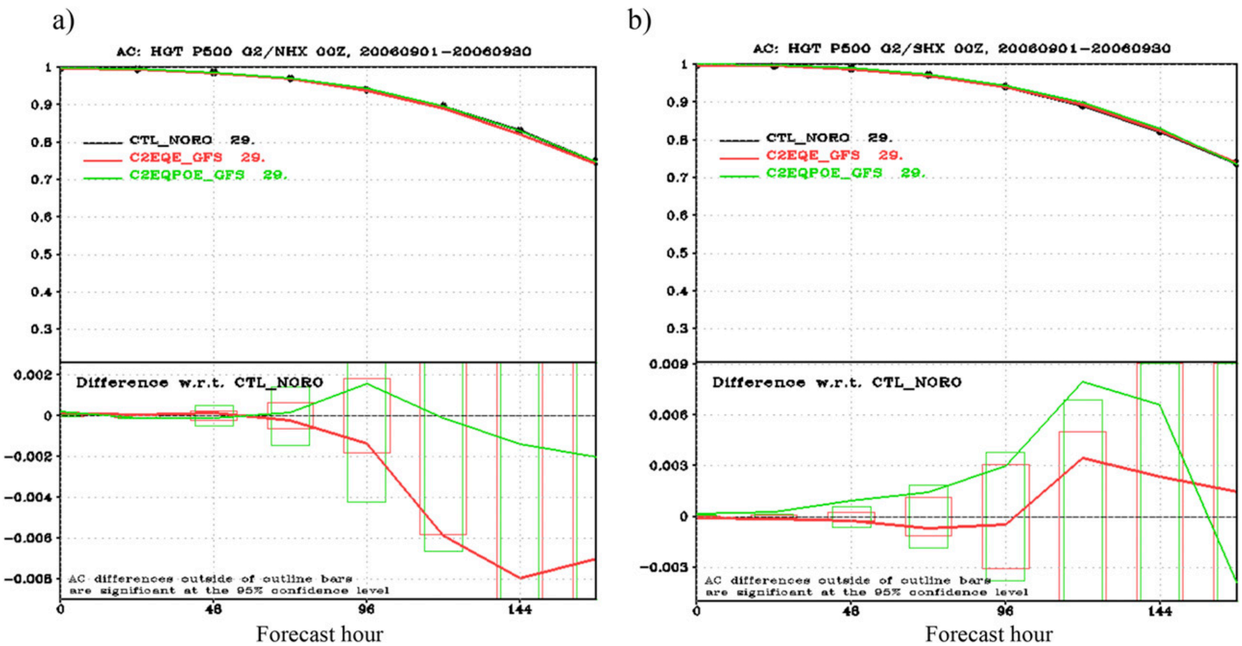

FIG. 8. Anomaly correlation score for the 500-hPa geopotential heights for CTL_NORO (black), C2EQE_GFS (red), and C2EQPOE_GFS (green) for the (a) Northern Hemisphere and (b) Southern Hemisphere. The lower parts of each panel show differences with respect to CTL_NORO, with positive being an improvement. Bars show limits of statistical significance at the 95% confidence level; values outside the bars are statistically significant.

refractivity are retrieved from profiles of bending angle with the use of auxiliary data. Typically, original measurements directly observed from a sensor are preferred over retrievals, as this prevents having to deal with additional retrieval and correlated observation errors. On the other hand, the larger variability of bending-angle profiles due to atmospheric vertical refractivity gradients makes it's assimilation more challenging. The assimilation of bending angles was shown to provide an overall slight improvement in global NWP skill at NOAA as compared to the assimilation of refractivity soundings (Cucurull et al. 2013). Earlier OSSEs with RO observations used refractivities because these algorithms are simpler to implement than a bending-angle simulator. To quantify to what extent OSSE results might have been modified due to a change on the simulated observation type, here we compare some of the earlier OSSEs with GFS and a refractivity forward operator described in Cucurull and Mueller (2020) with the runs analyzed in section 4a. Both the equatorial and the equatorial and polar components combined are investigated. For consistency with the naming convention adopted in the present paper and because the symbol usually used for refractivity is *n*, experiments from Cucurull and Mueller (2020) are renamed here as C2EQE_NGFS (equatorial component) and C2EQPOE_NGFS (equatorial and polar components combined).

Anomaly correlation score for the 500-hPa geopotential heights as a function of forecast lead time for the equatorial RO observations is shown in Figs. 10a and 10b for the NH and SH, respectively. The only difference between C2EQE_NGFS and C2EQE_GFS is the forward operator, and associated observation type and error, used in the assimilation experiments. Differences between these experiments and a control experiment without RO are in general not statistically significant, except for the first three days in the SH, where the use of refractivity profiles seems to slightly degrade skill in the SH (Fig. 10b). In general, the assimilation of bending-angle profiles seems to perform slightly better than the assimilation of refractivity in the SH, while the opposite is true in the NH.

The assimilation of soundings of refractivity in the combined C2EQPOE_NGFS improves skill over the control in the NH, although results are not statistically significant past day 4 (Fig. 10c). The use of bending angle versus refractivity is overall neutral. Although the assimilation of either refractivity or bending-angle soundings results in a positive impact in the SH, the use of refractivity outperforms the impact of assimilating bending angles (Fig. 10d). Since the assimilation of bending angles is more challenging than the assimilation of refractivity soundings, and the quality control procedures and observation errors have not been updated at NCEP in several years, this counterintuitive finding indicates that the assimilation of bending angles at NCEP requires further tuning to improve performance.

Nevertheless, all RO impacts from this section combined with the findings in section 4a are smaller than the RO impacts in section 3, suggesting that the impact of changing the RO forward operator from a one-dimensional refractivity to a one-dimensional bending angle is smaller than the impact of model configuration changes. Although not tested

Brought to you by NOAA Central Library | Unauthenticated | Downloaded 01/25/21 09:15 PM UTC

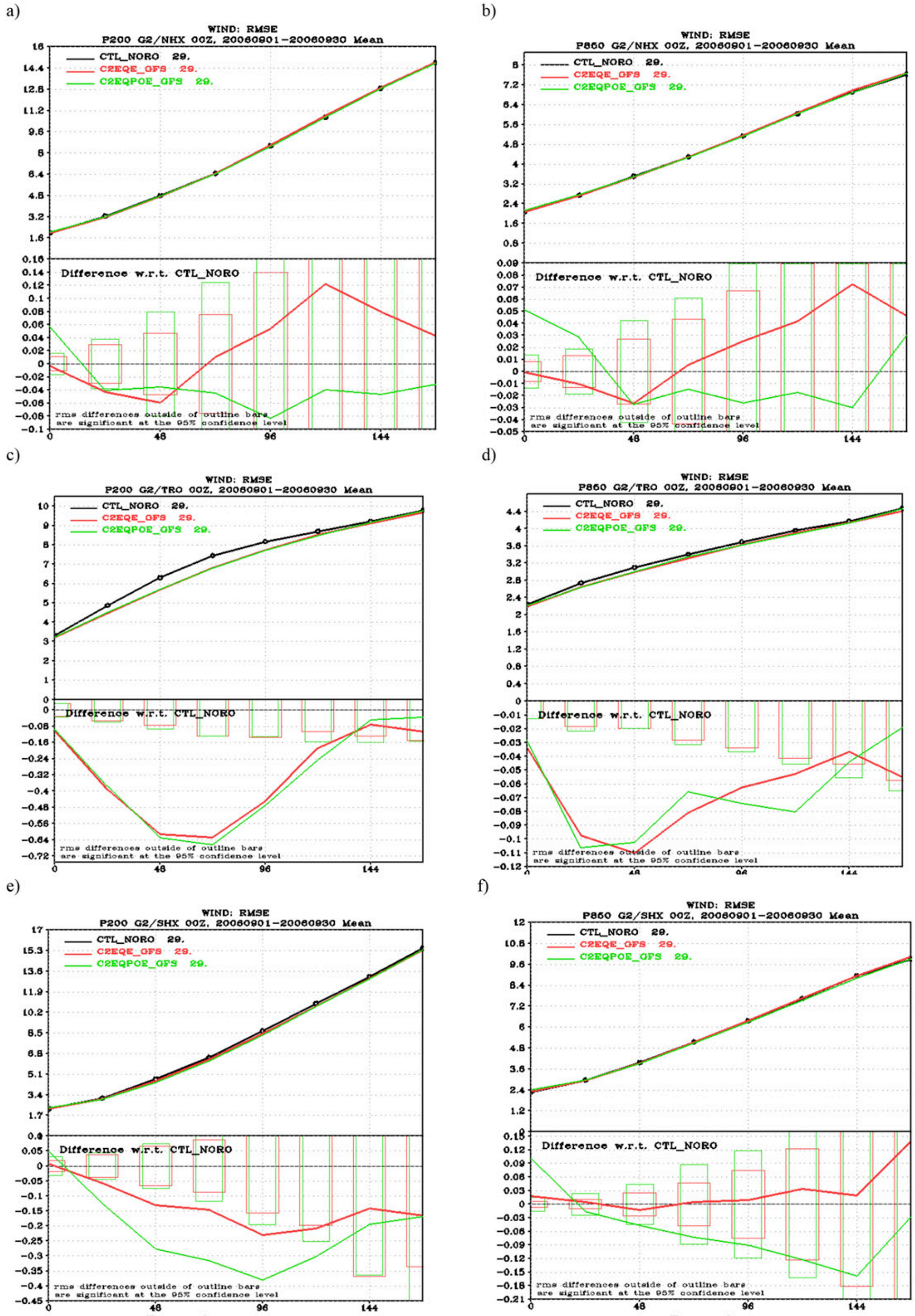

FIG. 9. (left) Upper (200 hPa) and (right) lower (850 hPa) root-mean-square wind errors ($\mathrm{m\,s^{-1}}$) for the (a),(b) Northern Hemisphere; (c),(d) tropics; and (e),(f) Southern Hemisphere as a function of the forecast hour for CTL_NORO (black), C2EQE_GFS (red), and C2EQPOE_GFS (green). The lower parts of each panel show differences with respect to CTL_NORO, with negative being an improvement. Bars show limits of statistical significance at the 95% confidence level; values outside the bars are statistically significant.

Brought to you by NOAA Central Library | Unauthenticated | Downloaded 01/25/21 09:15 PM UTC

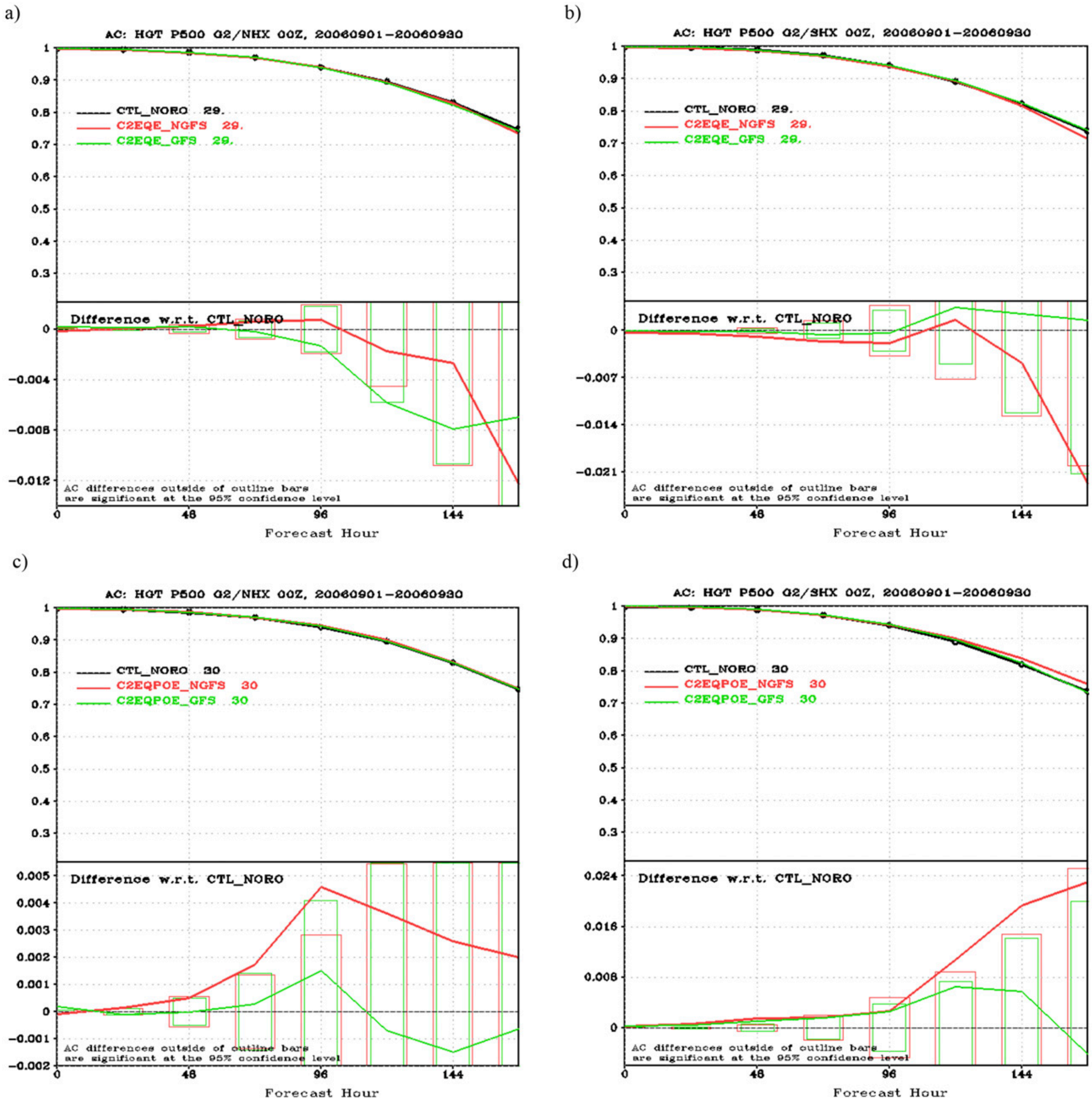

FIG. 10. Anomaly correlation score for the 500-hPa geopotential heights as a function of the forecast lead time for CTL_NORO (black), C2EQE_NGFS (red), and C2EQE_GFS (green) for the (a) Northern Hemisphere and (b) Southern Hemisphere. Corresponding values for all of the COSMIC-2 equatorial and polar observations combined observations are shown for CTL_NORO (black), C2EQPOE_NGFS (red), and C2EQPOE_GFS (green) for (c) Northern Hemisphere and (d) Southern Hemisphere. The lower parts of each panel show differences with respect to CTL_NORO, with positive being an improvement. Bars show limits of statistical significance at the 95% confidence level; values outside the bars are statistically significant.

in this study, it is very unlikely that the use of refractivity would overperform the use of bending angle in the FV3GFS configuration, at least for most verification metrics, because there were no changes in the conversion from GFS to FV3GFS directly related to the assimilation of RO observations.

Small differences exist for RMS wind errors as well (not shown). In general, the assimilation of the equatorial RO observations shows small sensitivity to the chosen forward operator and observation type. Small differences with the equatorial observations only exist in the lower levels, where the bending-angle forward operator results in slightly lower RMS wind errors in the tropics and SH. When both equatorial and polar observations are combined, small differences exist in the upper level NH and lower level SH RMS

Brought to you by NOAA Central Library | Unauthenticated | Downloaded 01/25/21 09:15 PM UTC

wind errors, with the use of refractivity resulting in slightly better results.

5. Conclusions

As data assimilation algorithms, model characteristics, including spatial and temporal resolution, and the observing system continues to evolve, it is necessary to repeat the most relevant OSSEs with these improved configurations to ensure that results continue to be valid for decision-making. Otherwise, we risk over or underestimating impacts of proposed observing technologies, providing information that might have become obsolete over time. In this study, we have investigated the impact of the originally proposed COSMIC-2 mission, with an equatorial and polar component, by using the current operational NWP system at NOAA and a one-dimensional bending-angle forward operator for the assimilation of RO observations.

Earlier findings indicating that globally distributed RO observations are more important than denser sampling of the tropical latitudes in order to improve weather prediction globally remain valid. Additional equatorial RO observations from low-inclination satellites supplementing the global coverage provided by satellites in high-inclination orbits produces further beneficial forecast impacts in the NH. On the other hand, no significant added benefits are seen in the SH. Overall, RO impact experiments conducted here show that the benefits from assimilating soundings of RO are more significant than the impacts found in previous OSSEs. This is encouraging since OSSEs conducted here used a more recent version of the operational data assimilation and forecast system at NOAA.

In these updated OSSEs, we have found that the impact of the equatorial component of the originally planned COSMIC-2 mission has significantly increased. Previous OSSEs had showed that benefits from the assimilation of equatorial RO observations were largely limited to tropical winds. The most relevant result of our investigation is that, while the lower inclination orbit component (now officially named COSMIC-2) had showed neutral impact over the extratropics in previous OSSE studies, significant positive impact is now found globally in terms of mass and wind fields. This change in impact is most significant in the NH.

It is important to note that, although COSMIC-2 data has recently been released to operational NWP centers, our study assumed final satellite orbit deployment, which is not expected until around May 2021. Exact level of performance of real observations (i.e., error characteristics and sounding quality) is never perfectly simulated in an OSSE framework, which might affect estimated impacts. Also, although it is unlikely that RO impacts might significantly change with the use of other higher-resolution global nature runs because of the large (~100 km) horizontal scale of RO measurements, this was not addressed here.

Furthermore, we have also investigated the impacts of using a new data assimilation and forecast system, and RO observation type and associated forward operator, on the original COSMIC-2 mission plan. No significant impact was found with the change of the one-dimensional RO forward operator. The impact from using a more recent data assimilation and forecast system was the largest contributor to changes in the OSSE results. More sophisticated RO forward operators that take into account horizontal gradients of atmospheric refractivity were not investigated here. However, we expect that these improved RO algorithms might play a more significant role, and they should be evaluated in future OSSE sensitivity studies.

Acknowledgments. The authors thank the NOAA OSSE team, who helped to develop and calibrate the OSSE system, and in particular Ruifang Li for her support in developing the bending-angle component. Three anonymous reviewers provided very helpful comments. Author Sean Casey was supported through the University of Miami/CIMAS Grant NA15OAR4320064NOAA.

Data availability statement. The dataset on which this paper is based is too large to be retained or publicly archived with available resources. Documentation and methods used to support this study are available from Dr. Lidia Cucurull (lidia.cucurull@noaa.gov) at the National Oceanic and Atmospheric Administration (NOAA).

REFERENCES

Anthes, R. A., and Coauthors, 2008: The COSMIC/FORMOSAT-3 mission: Early results. *Bull. Amer. Meteor. Soc.*, **89**, 313–334, https://doi.org/10.1175/BAMS-89-3-313.

Bonavita, M., 2014: On some aspects of the impact of GPSRO observations in global numerical weather prediction. *Quart. J. Roy. Meteor. Soc.*, **140**, 2546–2562, https://doi.org/10.1002/qj.2320.

Boukabara, S.-A., and Coauthors, 2018: Community Global Observing System Simulation Experiment (OSSE) Package (CGOP): Perfect observations simulation validation. *J. Atmos. Oceanic Technol.*, **35**, 207–226, https://doi.org/10.1175/JTECH-D-17-0077.1.

Casey, P. F., L. Cucurull, and A. Vidal, 2019: Global OSSE systems capabilities at NOAA. *2019 Fall Meeting*, San Francisco, CA, Amer. Geophys. Union, Abstract A24E-08, https://agu.confex.com/agu/fm19/meetingapp.cgi/Paper/539812.

Cucurull, L., 2010: Improvement in the use of an operational constellation of GPS radio-occultation receivers in weather forecasting. *Wea. Forecasting*, **25**, 749–767, https://doi.org/10.1175/2009WAF2222302.1.

——, and R. A. Anthes, 2014: Impact of infrared, microwave, and radio occultation satellite observations on operational numerical weather prediction. *Mon. Wea. Rev.*, **142**, 4164–4186, https://doi.org/10.1175/MWR-D-14-00101.1.

——, and M. J. Mueller, 2020: An analysis of alternatives for the COSMIC-2 constellation in the context of global observing system simulation experiments. *Wea. Forecasting*, **35**, 51–66, https://doi.org/10.1175/WAF-D-19-0185.1.

——, J. C. Derber, and R. J. Purser, 2013: A bending angle forward operator for global positioning system radio occultation measurements. *J. Geophys. Res. Atmos.*, **118**, 14–28, https://doi.org/10.1029/2012JD017782.

——, R. A. Anthes, and L.-L. Tsao, 2014: Radio occultation observations as anchor observations in numerical weather prediction models and associated reduction of bias corrections in microwave and infrared satellite observations.

Brought to you by NOAA Central Library | Unauthenticated | Downloaded 01/25/21 09:15 PM UTC

J. Atmos. Oceanic Technol., **31**, 20–32, https://doi.org/10.1175/JTECH-D-13-00059.1.

——, R. Li, and T. Peevey, 2017: Assessment of radio occultation observations from the COSMIC-2 mission with a simplified observing system simulation experiment configuration. *Mon. Wea. Rev.*, **145**, 3581–3597, https://doi.org/10.1175/MWR-D-16-0475.1.

——, R. Atlas, R. Li, M. Mueller, and R. N. Hoffman, 2018: An observing system simulation experiment with a constellation of radio occultation satellites. *Mon. Wea. Rev.*, **146**, 4247–4259, https://doi.org/10.1175/MWR-D-18-0089.1.

——, K. Rosado, R. A. Anthes, and R. J. Purser, 2020: RO data exploitation to optimize impact of COSMIC-2 to improve global and hurricane numerical weather forecasts at NOAA. *10th Conf. on Transition of Research to Operations*, Boston, MA, Amer. Meteor. Soc., 4.1, https://ams.confex.com/ams/2020Annual/webprogram/Paper365357.html.

Dee, D. P., 2005: Bias and data assimilation. *Quart. J. Roy. Meteor. Soc.*, **131**, 3323–3343, https://doi.org/10.1256/qj.05.137.

Errico, R. M., R. Yang, N. Prive, K.-S. Tai, R. Todling, M. E. Sienkiewicz, and J. Guo, 2013: Development and validation of observing-system simulation experiments at NASA's Global Modeling and Assimilation Office. *Quart. J. Roy. Meteor. Soc.*, **139**, 1162–1178, https://doi.org/10.1002/qj.2027.

Hoffman, R. N., and R. Atlas, 2016: Future observing system simulation experiments. *Bull. Amer. Meteor. Soc.*, **97**, 1601–1616, https://doi.org/10.1175/BAMS-D-15-00200.1.

Kursinski, E. R., G. A. Hajj, J. T. Schofield, R. P. Linfield, and K. R. Hardy, 1997: Observing Earth's atmosphere with radio occultation measurements using the Global Positioning System. *J. Geophys. Res.*, **102**, 23 429–23 465, https://doi.org/10.1029/97JD01569.

Melbourne, W. G., and Coauthors, 1994: The application of spaceborne GPS to atmospheric limb sounding and global change monitoring. Jet Propulsion Laboratory Tech. Rep. 94-18, 158 pp.

Putman, W., A. M. da Silva, L. E. Ott, and A. Darmenov, 2014: Model configuration for the 7- km GEOS-5 nature run, Ganymed release (non-hydrostatic 7 km global mesoscale simulation). NASA GMAO Office Note 5 (version 1.0), 18 pp., http://gmao.gsfc.nasa.gov/pubs/docs/Putman727.pdf.

——, A. Darmenov, A. da Silva, R. Gelaro, A. Molod, L. Ott, and M. J. Suarez, 2015: A 7-km non-hydrostatic global mesoscale simulation for OSSEs with the Goddard Earth Observing System model (GEOS-5). *19th Conf. on Integrated Observing and Assimilation Systems for the Atmosphere, Oceans, and Land Surface (IOAS-AOLS)*, Phoenix, AZ, Amer. Meteor. Soc., 3.1, https://ams.confex.com/ams/95Annual/webprogram/Paper260701.html.

Rocken, C., and Coauthors, 1997: Analysis and validation of GPS/MET data in the neutral atmosphere. *J. Geophys. Res.*, **102**, 29 849–29 866, https://doi.org/10.1029/97JD02400.

Brought to you by NOAA Central Library | Unauthenticated | Downloaded 01/25/21 09:15 PM UTC